

Direct Preparation of the Nanocrystalline MnZn Ferrites by Using Oxalate as Precipitant

Fei Hua^{1,2}, Cuicui Yin¹, Huanque Zhang³, Qiangqiang Suo³, Xin Wang¹, Huifen Peng¹

¹School of Materials Science & Engineering, Hebei University of Technology, Tianjin, China

²Department of Fire Protection Engineering, Chinese People's Armed Police Force Academy, Langfang, China

³School of Chemical Engineering, Hebei University of Technology, Tianjin, China

Email: hpeng226@163.com

Received 28 September 2015; accepted 10 December 2015; published 17 December 2015

Abstract

Oxalate was generally used as a precipitant for synthesis of MnZn ferrites during the co-precipitation process. However, the MnZn ferrite couldn't be directly obtained and a calcination process was needed. In this research, we reported a direct preparation of the MnZn ferrite nanoparticles by using co-precipitation method, together with refluxing process. XRD measurements proved that crystallite size of the obtained samples increased with an increase in pH value of the co-precipitation solution, and that the crystallite size of about 25 nm was obtained for the sample at a pH of 13. This sample showed the maximum M_s of 58.6 emu/g, which was about one times larger than that of 12 (pH value). Calcination to the obtained samples result in an enlargement in their crystal size and an improvement in their magnetic properties with an increase in temperatures. The samples calcinated in $\text{CO}_2 + \text{H}_2$ atmosphere presented good stability, and the maximum M_s value of 188.2 emu/g was obtained for the 1100°C-heated sample. Unfortunately, precipitation of some Fe_2O_3 at 800°C suggested poor stability of the nanocrystalline MnZn ferrite in N_2 atmosphere.

Keywords

Magnetic Material, MnZn Ferrite, Co-Precipitation Process, Nanocrystalline Material

1. Introduction

MnZn ferrite is one of the most important soft ferrites, which present high magnetic permeability, high saturation magnetization, high resistivity, low coercivity, low power losses and so on [1]. It is widely used in many fields, such as deflection yoke rings, computer memory chips, magnetic recording heads, microwave devices, transducers, transformers and so on [2]. Additionally, nano-sized MnZn ferrite is a good candidate for biomedical purposes, including magnetically guided drug delivery and magnetic resonance image [3], because of its high magnetic moment, good chemical stability and reactive surfaces when attaching to biological molecules [4].

Ferrite is usually synthesized by the conventional ceramic technique, where high temperature is needed in order for enough solid-state reactions between raw materials, large and inhomogeneous particles, together with

some impurities, greatly restrict magnetic properties of the products [5]-[7]. Therefore, wet chemical synthesis like co-precipitation [8]-[10], sol-gel [11] [12], hydrothermal method [13], and micro-emulsion process [14] [15] is expected for the production of ferrites with excellent magnetic properties. Among these methods, co-precipitation process is often used to the preparation of the homogeneous ferrite nanoparticles [4]. During this process, oxalate is generally used as a precipitant to prepare the ferrite powder. Angerman *et al.* [16] reported that β -oxalate with orthorhombic structure was formed when precipitating at room temperature, and that monoclinic α -oxalate was obtained at 90°C. Those oxalates could be completely transformed to ferrite when decomposition at 650°C [17]. On the other hand, Fritsch *et al.* [18] found that Mn-riched ferrite ($\text{Fe}_{3-x}\text{Mn}_{x\Box 3\delta/4}\text{O}_{4+\delta}$) with $x > 1.5$ presented complex structures like cubic, tetragonal or a mixture of them. This phenomenon should be attributed to the lack of miscibility at low temperature in the Fe_3O_4 - Mn_3O_4 system. In this paper, nanocrystalline MnZn ferrite was directly synthesized at room temperature by using the co-precipitation method, followed by a refluxing process. We investigated structures of the products and their phase transitions during heating under different atmosphere.

2. Experimental

2.1. Sample Preparation

Reagent-grade $\text{FeCl}_3 \cdot 6\text{H}_2\text{O}$ (Bodi Chemical, Tianjin, 99%), $\text{ZnSO}_4 \cdot 7\text{H}_2\text{O}$ (Bodi Chemical, Tianjin, 99.5%), $\text{MnSO}_4 \cdot \text{H}_2\text{O}$ (Bodi Chemical, Tianjin, 99%) were used as starting materials. Reagent-grade $(\text{NH}_4)_2\text{C}_2\text{O}_4 \cdot \text{H}_2\text{O}$ (Fengchen Chemical, Tianjin, 99.8%) and NaOH (Bodi Chemical, Tianjin, 99%) were used as co-precipitants, they were dissolved into de-ionized water at a concentration of 0.2mol/L and 6mol/L, respectively. $\text{NH}_3 \cdot \text{H}_2\text{O}$ (Fengchen Chemical, Tianjin, 25%) was used during precipitation at a concentration of about 5%.

The starting materials were weighed according to the formula $\text{Mn}_{0.7}\text{Zn}_{0.2}\text{Fe}_{2.1}\text{O}_4$. Suitable $(\text{NH}_4)_2\text{C}_2\text{O}_4 \cdot \text{H}_2\text{O}$ and $\text{NH}_3 \cdot \text{H}_2\text{O}$ were initially added into 0.1 mol/L $\text{FeCl}_3 \cdot 6\text{H}_2\text{O}$ solution under constant magnetic stirring to remain pH value of the solution at about 4. Then 0.9 mol/L $\text{MnSO}_4 \cdot \text{H}_2\text{O}$ and 0.2 mol/L $\text{ZnSO}_4 \cdot 7\text{H}_2\text{O}$ were introduced to the above solution. The $(\text{NH}_4)_2\text{C}_2\text{O}_4 \cdot \text{H}_2\text{O}$ and $\text{NH}_3 \cdot \text{H}_2\text{O}$ were re-added into the solution till its pH value of 8.5. At last, NaOH was added to the solution until its pH value of 13. Then the solution was refluxed for 7 h. The obtained precipitated product was washed with distilled water until a clear solution, and then dried at 80°C for 7 h. The dried powder was calcinated between 400°C to 1200°C under different atmosphere.

2.2. Sample Characterization

X-ray diffraction (XRD) patterns were recorded at room temperature with a Bruker AXS X-ray diffractometer using a Cu-K α radiation at a continuous scanning rate of 10 min⁻¹ in the 2θ range of 10° to 90°. Crystallite size of the samples was calculated according to (311) peak in the XRD patterns using the Debye-Scherrer's equation:

$$D = 0.94\lambda / \beta \cos\theta \quad (1)$$

where λ is the X-ray wavelength, θ is Bragg's angle and β is full width at half the maxima (FWHM). The saturation magnetization M_s , remanence magnetization, M_r , and coercive force, H_c , of the samples were calculated in terms of hysteresis loops measured by LakeShore-7400 vibrating sample magnetometer (VSM). In order to identify possible phase transformation in samples, the TG/DTA measurements were conducted in N_2 between 25°C and 1200°C at a rate of 10°C min⁻¹ using a Thermo Analyzer (TA, SDT-DTA 2960).

3. Results and Discussion

Figure 1 shows XRD patterns of as-synthesized samples, of which XRD peaks match well with those of the spinel MnZn ferrite (JCPDS No.74-2402). Almost no other peaks are found in the XRD patterns. Those results suggest that the samples prepared at different pH values are pure MnZn ferrite with spinel structure. In addition, apparent widening in the XRD peaks indicates a nano-scale crystallit size in those samples, and the narrower XRD peaks suggest that the crystals enlarge with an increase in the pH values (about 17 nm at pH of 12, and 25 nm at pH of 13).

Figure 2 shows the measured room-temperature hysteresis loops of the samples in **Figure 1**. Upon increasing pH values in the co-precipitation solutions, the saturation magnetization, M_s , apparently increase. And the

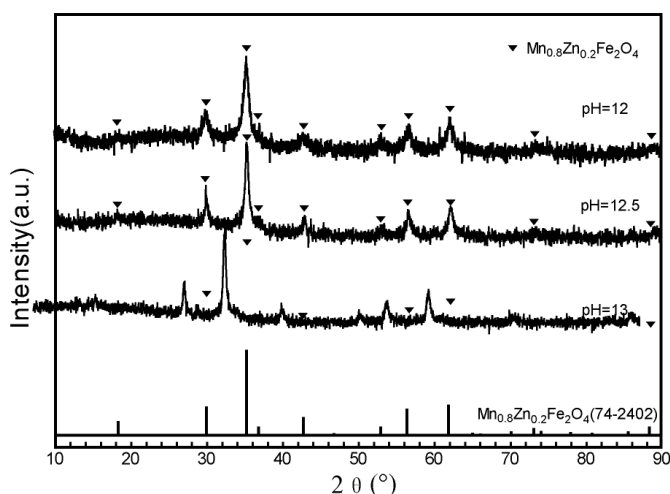


Figure 1. XRD patterns for the samples synthesized at various pH values.

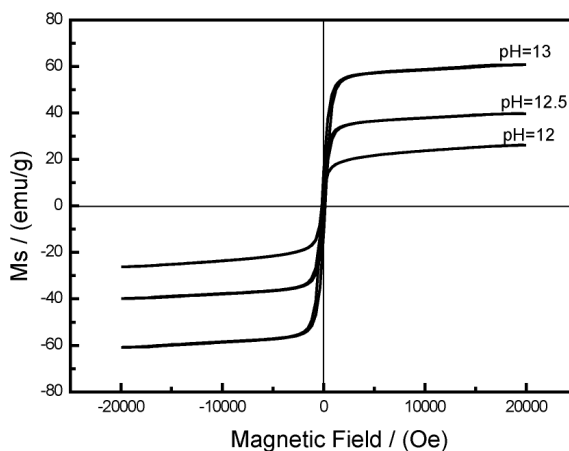


Figure 2. Magnetic hysteresis loops for the samples in **Figure 1**.

maximum M_s of 58.6 emu/g is obtained in the sample at a pH of 13. This M_s value is almost the highest one reported recently [5] [19]-[22], is about one times larger than that of pH = 12. Similar results were reported by Narasimhan *et al.* [23].

It is known that magnetism of the powdered MnZn ferrite is tightly related to its crystal size. Szczygiel *et al.* [24] found that superparamagnetism occurred in the MnZn ferrite powder with its crystal size less than 10 nm. Therefore, decrease in M_s with decrease in pH value should be attributable to the decrease in the crystallite size of the samples in the present research.

It is reported that MnZn ferrite cannot be directly obtained by using oxalate as precipitant during the co-precipitation process, and that heat treatment at certain temperature is generally needed to precursor [16] [22]. Results obtained in the present research not only simplify the preparation process of the MnZn ferrite, but also improve its quality because inclusion is easily produced during the heat treatment.

Figure 3 shows thermal analysis curves of the sample prepared at pH of 13. Total mass loss of the sample is about 8% during heating between room temperature and 1000°C, and the sharp mass loss occurring below 400°C should be attributable to evaporation of the adsorbed water and the crystallized water contained in the sample. No apparent endothermal or exothermal peaks are found in the DTA curves. Those results further prove that the samples prepared in this research are pure MnZn ferrite.

The MnZn ferrite is generally used in the bulk state, and then a sintering process is needed for the powdered one. However, the MnZn ferrite is reported to easily decompose according to Equation (2) in a heated state

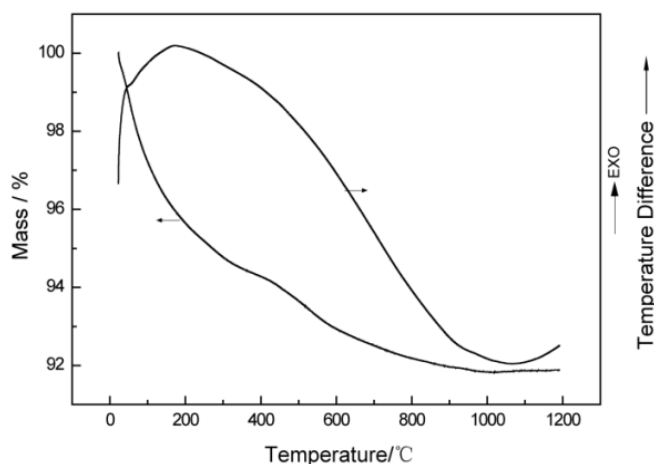
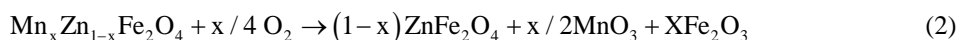


Figure 3. TG and DTA curves measured in N_2 for the sample at pH of 13.

under the oxidation atmosphere [2], and precipitation of Fe_2O_3 greatly deteriorates its magnetic properties.



Accordingly, we investigate phase transitions and variation in magnetic properties of the prepared samples during calcinations. **Figure 4** shows XRD patterns of the calcinated samples under different atmosphere. XRD patterns of the uncalcinated ones are also presented in this figure for comparison. Under certain atmosphere, XRD peaks of the sample become stronger in intensity and narrower in width, followed by a gradual color variation from brown to dark brown, with an increase in the calcination temperature. It is noteworthy that some XRD peaks attributable to Fe_2O_3 , concomitant with a reddish color in sample, appear in the XRD pattern of the sample calcinated at $800^\circ C$ under N_2 atmosphere. Further calcination at high temperature results in disappearance of those XRD peaks. Precipitation of some Fe_2O_3 from the MnZn ferrite may result from a little oxygen existing in the N_2 atmosphere. In contrast, the $CO_2 + H_2$ atmosphere is favorable to remain stability of the MnZn ferrite.

The measured hysteresis loops of the samples corresponding to those in **Figure 4** are shown in **Figure 5**. Their magnetization nearly saturates at the maximum field of 20 kOe, the magnetic parameters like M_s , M_r and H_c calculated according to **Figure 5** are presented in **Table 1**. Decrease in M_s with an increase in the calcination temperature below $800^\circ C$ under N_2 atmosphere should be related to decomposition of the MnZn ferrite or precipitation of non-magnetic Fe_2O_3 , shown in **Figure 4(a)**. Solution of the Fe_2O_3 into the MnZn ferrites at $1000^\circ C$ results in a sharp increase in M_s from 27.1 to 80.3 emu/g. On the other hand, the M_s gradually increases with an increase in the calcination temperature below $1100^\circ C$ for the samples calainated under $CO_2 + H_2$ atmosphere, concomitant with a decrease in H_c . The highest M_s of 188.2 emu/g is obtained for the sample, with the crystallite size of about 68.1 nm, calcinated at $1000^\circ C$. This is consistent with growth in crystallite size of samples during the calcination. The sharp decrease in M_s at $1200^\circ C$ is perhaps related to evaporation of some elements like Zn at high temperate. The M_s of the samples under $CO_2 + H_2$ is larger than that of N_2 at same calcinations temperature.

4. Conclusion

MnZn ferrite nanoparticles could be directly prepared by using co-precipitation and then refluxing process. Crystallite size of the obtained samples increased with an increase in pH value of the co-precipitation solution, and that the crystallite size of about 25 nm was obtained for the sample at a pH of 13. This sample also showed the maximum M_s of 58.6 emu/g, which was about one times larger than that of 12 (pH value). Calcination to the obtained samples resulted in an enlargement in their crystal size and an improvement in magnetic properties with an increase in temperatures. The samples calcinated in $CO_2 + H_2$ atmosphere presented good stability, and the maximum M_s of 188.2 emu/g was obtained for the sample heated at $1100^\circ C$. Unfortunately, precipitation of some Fe_2O_3 at $800^\circ C$ suggested poor stability of the nanocrystalline MnZn ferrite in N_2 atmosphere.

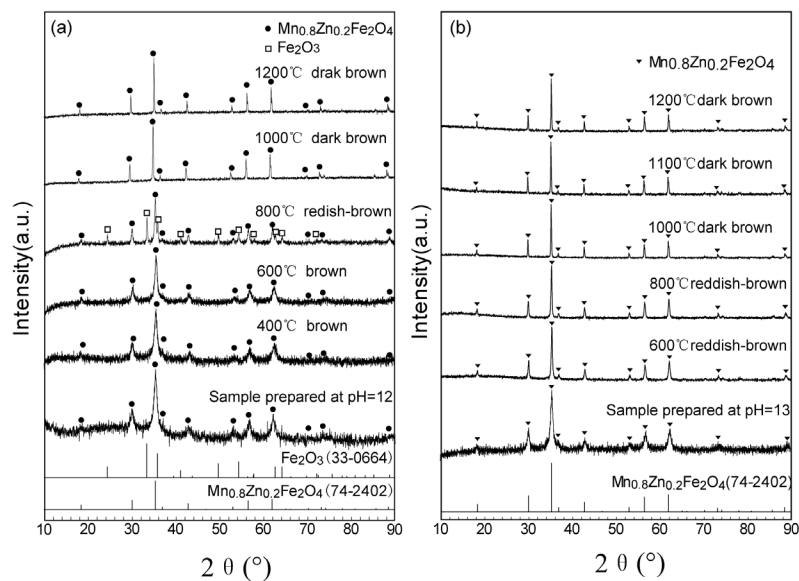


Figure 4. XRD patterns of the samples under different temperatures, (a) N_2 and (b) $CO_2 + H_2$.

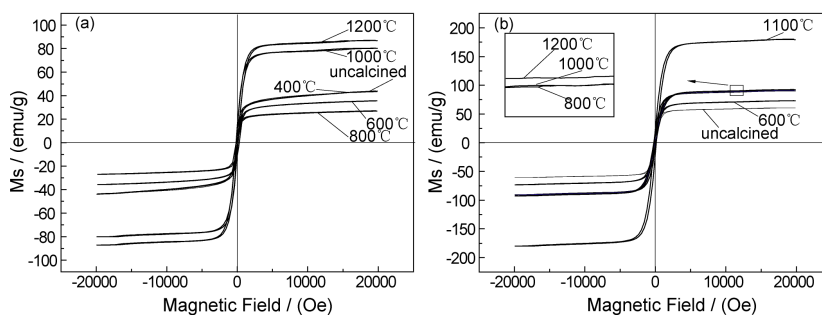


Figure 5. Hysteresis loops of the samples corresponding to those in **Figure 4**, (a) N_2 and (b) $CO_2 + H_2$.

Table 1. Magnetic properties of the samples calculated in terms of **Figure 5**.

atmosphere	Calcined Temperature T (°C)	M_s (emu/g)	H_c (Oe)	M_r (emu/g)	Crystallite size (nm)
N_2	400	43.9	118.4	7.3	32.9
	600	35.7	80.1	4.0	18.5
	800	27.1	58.4	2.2	26.0
	1000	80.3	135.1	11.4	52.8
	1200	87.2	123.6	9.8	81.6
	$CO_2 + H_2$	600	73.1	195.3	14.1
800		90.9	175.7	17.2	33.5
1000		90.8	128.1	9.0	63.4
1100		180.2	128.6	18.9	68.1
	1200	92.6	126.1	9.0	69.3

Acknowledgements

This work was supported by Tianjin Research Program of Application Foundation and Advanced Technology (major project) under a contract No.15JEZDJC31000.

References

- [1] Hu, P., Yang, H.B., Pan, D.A., Wang, H., Tian, J.J., Zhang, S.G., Wang, X.F. and Volinsky, A.A. (2010) Heat Treatment Effects on Microstructure and Magnetic Properties of Mn-Zn Ferrite Powders. *J. Magn. Magn. Mater.*, **322**, 173-177. <http://dx.doi.org/10.1016/j.jmmm.2009.09.002>
- [2] Waqas, H. and Qureshi, A.H. (2010) Low Temperature Sintering Study of Nanosized Mn-Zn Ferrites Synthesized by Sol-Gel Auto Combustion Process. *J. Therm. Anal. Calorim.*, **100**, 529-535. <http://dx.doi.org/10.1007/s10973-009-0590-6>
- [3] Šepelak, V., Heitjans, P. and Becker, K.D. (2007) Nanoscale Spinel Ferrites Prepared by Mechanochemical Route. *J. Therm. Anal. Calorim.*, **90**, 93-97. <http://dx.doi.org/10.1007/s10973-007-8481-1>
- [4] Sharifi, I., Shokrollahi, H. and Amiri, S. (2012) Ferrite-Based Magnetic Nanofluids Used in Hyperthermia Applications. *J. Magn. Magn. Mater.*, **324**, 903-915. <http://dx.doi.org/10.1016/j.jmmm.2011.10.017>
- [5] Zhang, C.F., Zhong, X.C., Yu, H.Y., Liu, Z.W. and Zeng, D.C. (2009) Effects of Cobalt Doping on the Microstructure and Magnetic Properties of Mn-Zn Ferrites Prepared by the Co-Precipitation Method. *Physica B: Condensed Matter*, **404**, 2327-2331. <http://dx.doi.org/10.1016/j.physb.2008.12.044>
- [6] Isfahani, M.J.N., Myndyk, M., Menzel, D., Feldhoff, A., Amighian, J. and Šepelak, V. (2009) Magnetic Properties of Nanostructured MnZn Ferrite. *J. Magn. Magn. Mater.*, **321**, 152-156. <http://dx.doi.org/10.1016/j.jmmm.2008.08.054>
- [7] Kadu, A.V., Jagtap, S.V. and Chaudhari, G.N. (2009) Studies on the Preparation and Ethanol Gas Sensing Properties of Spinel $Zn_{0.6}Mn_{0.4}Fe_2O_4$ Nanomaterials. *Curr. Appl. Phys.*, **9**, 1246-1251. <http://dx.doi.org/10.1016/j.cap.2009.02.001>
- [8] Jeyadevan, B., Tohji, K., Nakatsuka, K. and Narayanasamy, A. (2000) Irregular Distribution of Metal Ions in Ferrites Prepared by Co-Precipitation Technique Structure Analysis of Mn-Zn Ferrite Using Extended X-Ray Absorption Fine Structure. *J. Magn. Magn. Mater.*, **217**, 99-105. [http://dx.doi.org/10.1016/S0304-8853\(00\)00108-6](http://dx.doi.org/10.1016/S0304-8853(00)00108-6)
- [9] Venkataraju, C., Sathishkumar, G. And Sivakumar, K. (2010) Effect of Nickel on the Electrical Properties of Nanostructured MnZn Ferrite. *J. Alloys Compd.*, **498**, 203-206. <http://dx.doi.org/10.1016/j.jallcom.2010.03.160>
- [10] Iqbal, M.A., Islam, M.U., Ali, I., Kan, H.M., Mustafa, G. and Ali, I. (2013) Study of Electrical Transport Properties of Eu^{+3} Substituted MnZn-Ferrites Synthesized by Co-Precipitation Technique. *Ceram. Int.*, **39**, 1539-1545. <http://dx.doi.org/10.1016/j.ceramint.2012.07.104>
- [11] Fan, J.W. and Sale, F.R. (1996) Analysis of Power Loss on Mn-Zn Ferrites Prepared by Different Processing Routes. *IEEE Trans. Magn.*, **32**, 4854-4856. <http://dx.doi.org/10.1109/20.539174>
- [12] Azadmanjiri, J. (2007) Preparation of Mn-Zn Ferrite Nanoparticles from Chemical Sol-Gel Combustion Method and the Magnetic Properties after Sintering. *J. Non-Cryst. Solids*, **353**, 4170-4173. <http://dx.doi.org/10.1016/j.jnoncrsol.2007.06.046>
- [13] Rozman, M. and Drogenik, M. (1995) Hydrothermal Synthesis of Manganese Zinc Ferrites. *J. Am. Ceram. Soc.*, **78**, 2449-2455. <http://dx.doi.org/10.1111/j.1151-2916.1995.tb08684.x>
- [14] Yener, D.O. (1988) Synthesis of Pure and Manganese-, Nickel-, and Zinc-Doped Ferrite Particles in Water-in-Oil Microemulsions. *J. Am. Ceram. Soc.*, **84**, 1987-1995. <http://dx.doi.org/10.1111/j.1151-2916.2001.tb00947.x>
- [15] Mathew, D.S. and Juang, R.S. (2007) An Overview of the Structure and Magnetism of Spinel Ferrite Nanoparticles and Their Synthesis in Microemulsions. *Chem. Eng. J.*, **129**, 51-65. <http://dx.doi.org/10.1016/j.cej.2006.11.001>
- [16] Angermann, A. and Töpfer, J. (2011) Synthesis of Nanocrystalline Mn-Zn Ferrite Powders through Thermolysis of Mixed Oxalates. *Ceram. Int.*, **37**, 995-1002. <http://dx.doi.org/10.1016/j.ceramint.2010.11.019>
- [17] Ghodake, S.A., Ghodake, U.R., Sawant, S.R., Suryavanshi, S.S. and Bakare, P.P. (2006) Magnetic Properties of Ni-CuZn Ferrites Synthesized by Oxalate Precursor Method. *J. Magn. Magn. Mater.*, **305**, 110-119. <http://dx.doi.org/10.1016/j.jmmm.2005.11.041>
- [18] Fritsch, S.G., Vigiúé, S. and Roussier, A. (1999) Structure of Highly Divided Nonstoichiometric Iron Manganese Oxide Powders $Fe_{3-x}Mn_{x/3\delta/4}O_{4+\delta}$. *J. Solid State Chem.*, **146**, 245-252. <http://dx.doi.org/10.1006/jssc.1999.8345>
- [19] Cao, X., Liu, G., Wang, Y., Li, J.H. and Hong, R. (2010) Preparation of Octahedral Shaped $Mn_{0.8}Zn_{0.2}Fe_2O_4$ Ferrites via Co-Precipitation. *J. Alloys Compd.*, **497**, L9-L12. <http://dx.doi.org/10.1016/j.jallcom.2010.03.011>
- [20] Arulmurugana, R., Vaidyanathana, G., Sendhilnathanb, S. And Jeyadevan, B. (2006) Mn-Zn Ferrite Nanoparticles for Ferrofluid Preparation: Study on Thermal-Magnetic Properties. *J Magn Magn Mater*, **298**, 83-94. <http://dx.doi.org/10.1016/j.jmmm.2005.03.002>
- [21] Meng, Y.Y., Liu, Z.W., Dai, H.C., Yu, H.Y., Zeng, D.C., Shukla, S. and Ramanujan, R.V. (2012) Structure and Magnetic Properties of Mn(Zn)Fe_{2-x}RE_xO₄ Ferrite Nano-Powders Synthesized by Co-Precipitation and Refluxing Method. *Powder Technol.*, **229**, 270-275. <http://dx.doi.org/10.1016/j.powtec.2012.06.050>
- [22] Angermann, A., Töpfer, J., Silva, K.L. and Becker, K.D. (2010) Nanocrystalline Mn-Zn Ferrites from Mixed Oxalates:

Synthesis, Stability and Magnetic Properties. *J. Alloys Compd.*, **508**, 433-439.

<http://dx.doi.org/10.1016/j.jallcom.2010.08.083>

- [23] Narasimhan, B.R.V., Prabhakar, S., Manohar, P. and Gnanam, F.D. (2002) Synthesis of Gamma Ferric Oxide by Direct Thermal Decomposition of Ferrous Carbonate. *Mater. Lett.*, **52**, 295-300.

[http://dx.doi.org/10.1016/S0167-577X\(01\)00409-8](http://dx.doi.org/10.1016/S0167-577X(01)00409-8)

- [24] Szczygiel, I., Winiarska, K., Bieńko, A., Suracka, K. and Koniarek, G.D. (2014) The Effect of the Sol-Gel Autocombustion Synthesis Conditions on the Mn-Zn Ferrite Magnetic Properties. *J. Alloys Compd.*, **604**, 1-7.

<http://dx.doi.org/10.1016/j.jallcom.2014.03.109>